Responds to the reviewer's comments:

We sincerely thank the reviewer for the valuable comments and suggestions concerning our manuscript entitled "The evolution of cloud microphysics upon aerosol interaction at the summit of Mt. Tai, China". These comments are valuable and helpful for revising and improving our paper. The responses to reviewers are in blue. The changes are marked in red in the revised manuscript.

Reviewer 1

General comments:

This study investigates aerosol-cloud-interactions (ACI) using measurements from the high mountain site of Mt. Tai in China. As limited studies of ACI exist from high altitude measurement stations in this region, the study can potentially provide some useful data about these complex processes to the scientific community. However, the methodologies employed within this manuscript to investigate ACI are questionable, and lacking the necessary in-depth analysis currently associated with probing ACI - one of the most challenging topics currently facing the climate community. A number of conclusions presented are unsupported by the data, and rather arbitrary in nature. Numerous statements throughout the manuscript are not persuasive or lack evidence. Furthermore, the manuscript is not organised very well and the language and grammar throughout is far from the quality required for a scientific publication. Given the large concerns associated with some of the methodologies applied, subsequent conclusions drawn, and the general quality of the text I recommend a major revision of the entire manuscript before consideration for publication.

Responds: We sincerely thank you for your pertinent comments and valuable suggestions. We have revised our manuscript based on the comments from the two reviewers. We polished the language in the revised manuscript.

Major comments:

When investigating ACI it is of crucial importance to separate the contributions of changes in both aerosol and meteorology on any observed or simulated cloud response; as performed in other studies of ACI in the scientific literature, e.g. Malavelle et al., 2017. There does not appear to have been any attempt to account for variations in the meteorology in this study. If any of the analysis related to ACI is to remain in the manuscript, the study should include, but not limited to, the following additional analysis:

Comment A:

A detailed description of the measurement station with regard to location of instruments and prevailing meteorology. A picture and/or schematic is required to put the results in context of the environment in which they were measured, in particular, statistics on the height of measurements in relation to cloud base/top.

Response: Thank you for your comment. We add two graphs (Fig. S1 and Fig. S2) and detailed descriptions of location of instruments and prevailing meteorology in section 2.1 of the revised manuscript (Page 3 Line 28 to Page 4 Line 6):

"From 17 June to 30 July 2018, 40 cloud events in total were monitored at the Shandong Taishan Meteorological Station at summit of Mt. Tai (Tai'an, China; 117°13' E, 36°18' N; 1545 m a.s.l.; Fig. S1).

Mt. Tai is the highest point in the central of North China Plain (NCP) and located within the transportation channel between the NCP and the Yangtze River Delta (Shen et al., 2019). The altitude of Mt. Tai is close to 1.6 km, which is close to the top of the planetary boundary layer in Central East China and usually sited for the characteristic of particles inputting to clouds (Hudson, 2007). Local cloud events frequently occurred at the summit of Mt. Tai, especially in summer. As shown in Fig. S2, the prevailing wind direction during this summer campaign is east wind (23.3%), southwest wind (22.8%) and south wind (21.9%), respectively. About 85.6% of wind speed was less than 8 m s^{-1}. While the monitored cloud events in the present study was mainly influence by south wind (34.7%) and southwest wind (22%). The arrangement of instruments was presented in Fig. S1(b).”

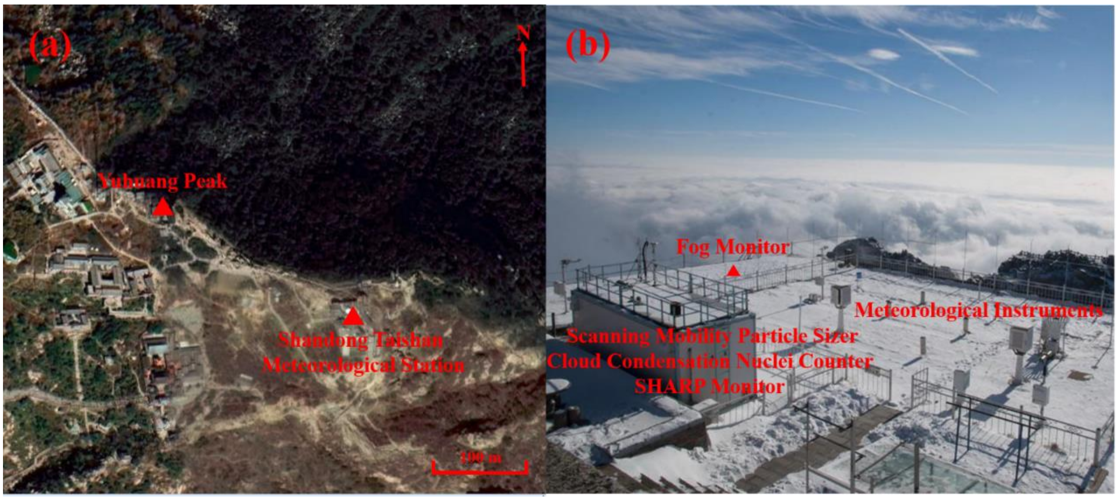

Figure S1. The pictures and schematic of (a) the measurement station (printscreen from Google Map) (b) the arrangement of instruments in Shandong Taishan Meteorological Station (http://p.weather.com.cn/2016/12/2638460.shtml). The corresponding sampling tubes were at least 1.5 m higher than the roof and at least 1.0 m away from each other to avoid the mutual interference.

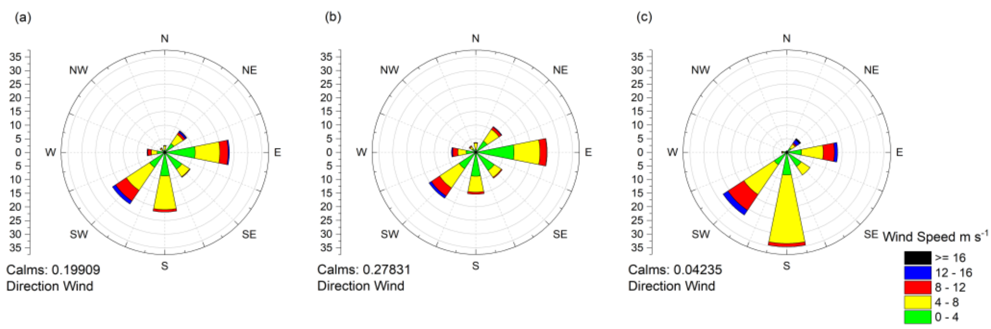

Figure S2. Wind direction and wind speed a) during the whole summer campaign at Mt. Tai, b) without cloud events and c) during cloud events.

Due to the lack of corresponding instruments, we cannot directly get the information of cloud base height (CBH) and cloud top height. Based on the meteorological data on the ground level, the lifting condensation level (LCL) was calculated and applied to approximate CBH as shown in Section 2.6. We added the information of CBH in Fig. 2b (Page 6 Line 12 - 23):

"2.6. Calculation of cloud base height

In the present study, the estimated lifting condensation level (LCL) is applied to represent the cloud base height (CBH) due to the lack of corresponding instruments. The calculation of LCL depends on the meteorological parameters measured at Tai'an Station. The ground-level data of temperature, dew point temperature, and pressure were used as input parameters (Georgakakos and Bras, 1984):

$$p_{LCL} = \frac{1}{\left(\frac{T_g - T_{gd}}{223.15} + 1\right)^{3.5}} \times p_g$$

$$T_{LCL} = \frac{1}{\left(\frac{T_g - T_{gd}}{223.15} + 1\right)} \times T_g$$

$$CBH = 18400 \times \left(1 + \frac{T_{LCL} - T_g}{273}\right) \times \lg \frac{p_g}{p_{LCL}}$$

Where p_{LCL} is the LCL pressure; T_{LCL} is the LCL temperature.

During the observation period, CBH ranged from 460.3 m to 3639.1 m with the average value of 1382.5 m. As shown in Fig. 2b, the observation station would be totally enveloped in clouds and around when cloud events occurred. The corresponding distance between the observation point and CBH was represented in Fig. 2b."

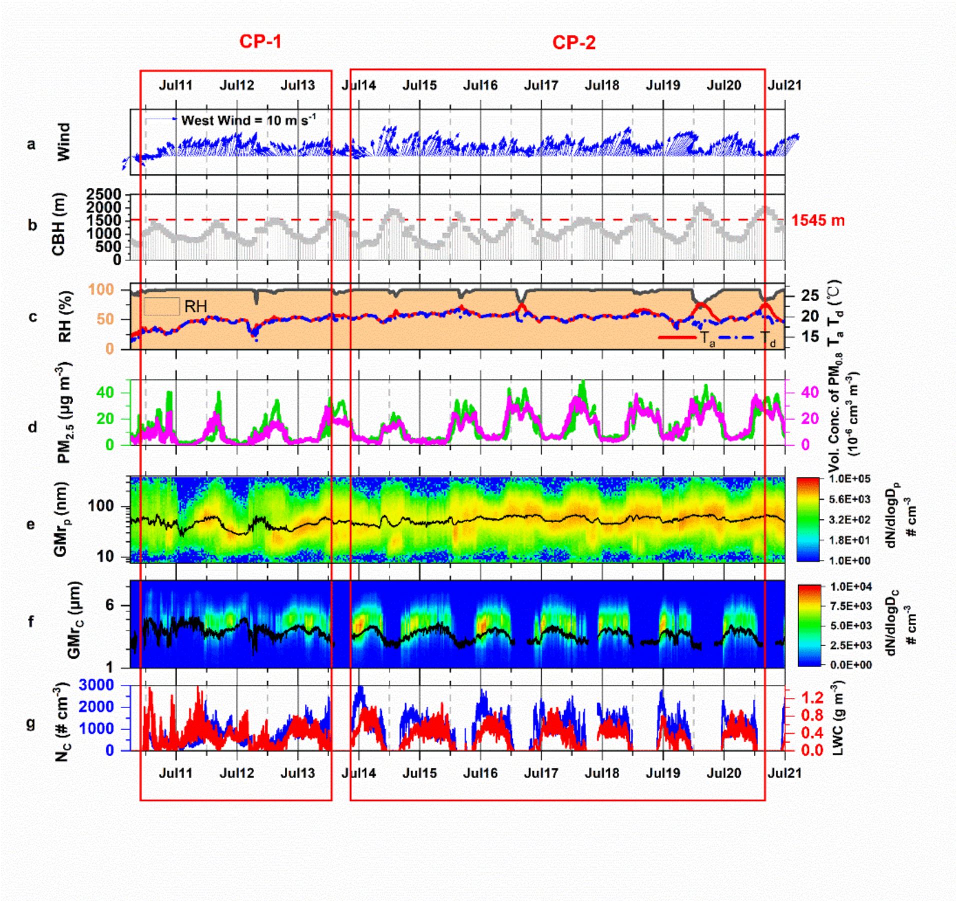

Figure 2: The monitoring information of CP-1 and CP-2. Including (a) Wind speed (WS, m s^{-1}) and wind direction (WD), (b) cloud based height (CBH, m) (c)relative humidity (RH, %), ambient temperature (T_a, ℃) and dew point temperature (T_d, ℃) (d) $PM_{2.5}$ mass concentrations (μg m^{-3}) and volumn concentration of $PM_{0.8}$ (10^{-6} cm^3 cm^{-3}) (e) size distribution of particles (13.6-763.5 nm) and corresponding geometric mean radius (GMr_P) (f) size distribution of cloud droplets (2-50 μm) and corresponding geometric mean radius (GMr_C) (g) N_C and LWC of cloud droplets.

Comment B:

Isolating the role of below cloud variations in meteorology, (updraft velocity) on incloud variations in supersaturation and cloud microphysical properties, e.g. cloud liquid water content; cloud droplet effective radius, cloud droplet number concentration. There is a vast amount of literature addressing this, e.g. Lance et al., 2004. If observations of cloud base updraft are not available, then alternative approaches should be sought, e.g. using a cloud model in conjunction with the in-cloud measurements to probe sensitivity to variations in meteorology in a robust manner.

Response: Thank you for your comment. Even though we do not have the observation data of updraft velocity, we assessed the influences of updraft velocity and topography on cloud microphysical properties during CP-1 and CP-2 based on the studies of Hammer et al. (2014) and Spiegel et al. (2012). Based on assumptions that air flow lines are parallel to the terrain and without occurrence of sideways convergence and divergence, updraft velocity was estimated by the horizontal wind speed (v_h) measured at the observation station Hammer et al. (2014):

$$v_{up} = \tan(\alpha) \times v_h$$

where α represented the inclination angle which was estimated from the altitudes of Tai'an City and the summit of Mt. Tai and the horizontal distance between them. For every cloud stages during CP-1 and CP-2, the transect direction of Mt. Tai was chosen based on the prevailing wind directions. For example, as shown in Fig. S3, the southwest-northeast transect of Mt. Tai was selected for CP-2 due to the prevailing wind direction of southwest wind. For the southwest-northeast transect of Mt. Tai, the horizontal distance between Tai'an City and the summit of Mt. Tai could be obtained from the Google Earth as about 7.2 km. The inclination angle, then, could be calculated to be about 10.6 °. It should be noticed that the calculated v_{up} could be considered as the upper limit of the true updraft velocity if the flow lines would not strictly follow the terrain Hammer et al. (2014). As shown in Table S2, the averaged values of v_{up} of different cloud stages during CP-1 and CP-2 did not change a lot. Even though updraft velocity could influence cloud microphysical properties, we think it did not hinder our discussion about CP-1 and CP-2 due to the small difference during the two cloud processes.

For estimating the influenced of wind direction and wind speed on Fog Monitor, Spiegel et al. (2012) calculated that the sampling efficiency (contributed by aspiration efficiency and transmission efficiency) under standard atmospheric conditions (p = 1013 mbar, T = 0 ℃) and represented the results in their Fig. 7. The sampling efficiency was depended on two parameters. One is sampling angle (θ_s) which is equal to α. The other is R_V which is equal to the velocity ratio of surrounding wind speed (U_0) with sampling speed (U) of FM-120:

$$R_V = \frac{U_0}{U} = \frac{\frac{v_h}{\cos(\alpha)}}{U}$$

Through calculation, the averaged R_V of CP-1 and CP-2 was 1.02 and 1.14, respectively. Thus, we could use Fig. 7a) from Spiegel et al. (2012), where R_V = 1.2, to estimate the sampling efficiency of FM-120 during CP-1 and CP-2. As can be seen, for θs = α = 10.6 °, the aspiration efficiency and transmission efficiency are all close to 1. Thus, we assumed that the influences of topography and updraft velocity on Fog Monitor were small and could be ignored during CP-1 and CP-2 (Page 4 Line 25 to Page 5 Line 16):

"The topography of the monitoring position could provide the vertical wind field (updraft velocity, v_{up}) and further affect cloud microphysical properties (Verheggen et al., 2007). Based on assumptions that air flow lines were parallel to the terrain and without occurrence of sideways convergence and divergence, v_{up} was estimated by the topography of Mt. Tai and the horizontal wind speed (v_h) measured at the observation station (Hammer et al., 2014), the calculation equation of was:

$$v_{up} = \tan(\alpha) \times v_h$$

Where α represented the inclination angle which was estimated from the altitudes of Tai'an City and the summit of Mt. Tai and the horizontal distance between them (Fig. S3). It should be noticed that the calculated v_{up} could be considered as the upper limit of the true updraft velocity if the flow lines would not strictly follow the terrain (Hammer et al., 2014). As shown in Table S2, the averaged v_{up} during two focused cloud processes (CP-1 and CP-2) studied in the present study was 0.82 m s^{-1} and 0.92 m s^{-1}, respectively, and did not change a lot. Thus, we simply assumed that the influence of v_{up} on cloud microphysical properties for CP-1 and CP-2 was the same.

In order to estimate the sampling losses due to wind speed and wind direction, the sampling efficiency (contributed by aspiration efficiency and transmission efficiency) was estimated based on the study of Spiegel et al. (2012). The sampling efficiency was depended on two parameters. One is sampling angle (θ_s) which is equal to α. The other is R_V which is equal to the velocity ratio of surrounding wind speed (U_0) with sampling speed (U) of FM-120:

$$R_V = \frac{U_0}{U} = \frac{\frac{v_h}{\cos(\alpha)}}{U}$$

In the study of Spiegel et al. (2012), they calculated that the sampling efficiency under standard atmospheric conditions (p = 1013 mbar, T = 0 °C) and represented the results in their Fig. 7. Through calculation, the averaged R_V of CP-1 and CP-2 was 1.02 and 1.14, respectively. Thus, we could use Fig. 7a) from Spiegel et al. (2012), where R_V = 1.2, to estimate the sampling efficiency of FM-120 during CP-1 and CP-2. As can be seen, for θs = α = 11.9° and 10.6° (Fig.S3), the aspiration efficiency and transmission efficiency are all close to 1. Thus, we assumed that the influences of topography and updraft velocity on Fog Monitor were small and could be ignored during CP-1 and CP-2."

Table S2. Estimated updraft velocity (V_{up}) (means ± S.D.), estimated cloud base height (CBH) (means ± S.D.) and the sensitivities analysis of N_C to N_P, CBH and v_{up} during CP-1 and CP-2.

	V_{up} m s^{-1}	CBH m	$^{a,b}\partial \ln N_C/\partial \ln N_P (R^2)$	$^{b}\partial \ln N_C/\partial \ln CBH (R^2)$	$^{b}\partial \ln N_C/\partial \ln v_{up} (R^2)$
CP-1	0.82 ± 0.29	1017.9 ± 301.5	0.544(0.2820)	-0.118(0.0018)	0.275(0.0599)
CP-2	0.92 ± 0.36	1040.4 ± 260.2	0.144(0.0500)	0.216(0.1279)	0.868(0.1167)

[a]The value of $\partial \ln N_C/\partial \ln N_P$ was equal to FIE_N

[b]R^2 represented correlation coefficient

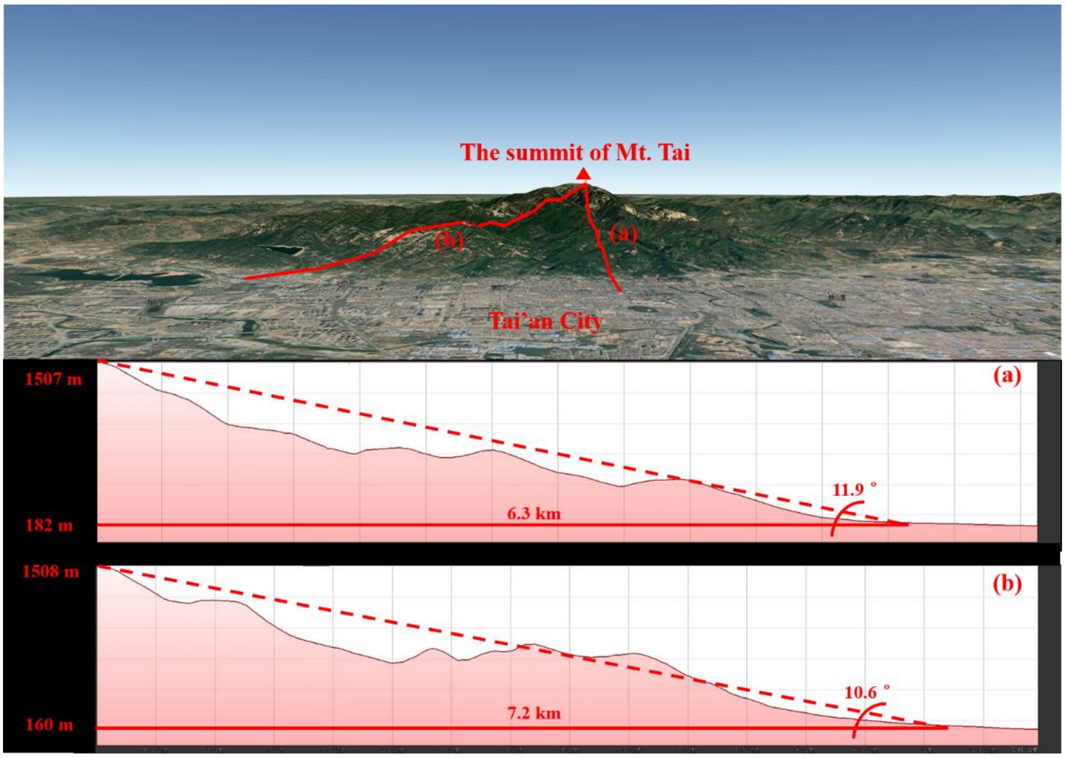

Figure S3. Influence of the topography on the vertical wind field at monitoring station. Taking (a) the south-north transect of Mt. Tai and (b) the southwest-northeast transect of Mt. Tai to estimate the inclination angles and updraft velocities.

Comment C:

Accounting for the role of measurement height relative to cloud base in analysis. The measured cloud microphysical properties will be strongly dependant at the height they are measured in relation to cloud-base. This needs to be accounted for in the data analysis prior to drawing conclusions regarding the role of aerosols on measured cloud properties.

Response: Thank you for your comment. We calculated the cloud base height (CBH) based on the estimation of the lifting condensation level (LCL) as shown in the response to Comment A. Then, we applied the equation as $S(CBH)=\partial lnN_c/\partial lnCBH$ to estimate the sensitivity of drop number concentration (N_C) to CBH. As shown in Table S2, Compared with CP-1 which was formed under relatively clean conditions, CP-2 was more sensitive to the change of CBH. We added the corresponding discussion in Page 10 Line 28 to Page 11 Line 6:

"In addition, the meteorological conditions and the topography during the monitoring period would also affect the microphysical properties of clouds. The sensitivity analysis of N_C to CBH and v_{up} was estimated by applying the equation as $S(X_i)=\partial lnN_C/\partial lnX_i$, where X_i represented CBH and v_{up}. As shown in Talbe S2, CP-2 was more sensitive to the variation of meteorological parameters if compared with CP-1. It was consistent with the study of McFiggans et al. (2006). They found that the sensitivity of N_C to v_{up} increased while the sensitivity of N_C to N_P decreased when N_P > 1000 # cm^{-3}. In the present study, the higher values of FIE_r and FIE_N of CP-1 indicated that if the same amount of aerosol particles entered the cloud, the size of cloud droplets in CP-1 would decrease more than that in CP-2. The albedo during CP-1 would be more susceptible to the change of aerosol particles. While the higher values of S(CBH) and S(v_{up}) of CP-2 indicated that CP-2 was more sensitive to the change of CBH and v_{up}. It might cause the periodical variations of cloud microphysical properties during CP-2."

Table S2. Estimated updraft velocity (V_{up}) (means ± S.D.), estimated cloud base height (CBH) (means ± S.D.) and the sensitivities analysis of N_C to N_P, CBH and v_{up} during CP-1 and CP-2.

	V_{up} m s^{-1}	CBH m	[a,b]$\partial lnN_C/\partial lnN_P(R^2)$	[b]$\partial lnN_C/\partial lnCBH(R^2)$	[b]$\partial lnN_C/\partial lnv_{up}(R^2)$
CP-1	0.82 ± 0.29	1017.9 ± 301.5	0.544(0.2820)	-0.118(0.0018)	0.275(0.0599)
CP-2	0.92 ± 0.36	1040.4 ± 260.2	0.144(0.0500)	0.216(0.1279)	0.868(0.1167)

[a]The value of $\partial lnN_C/\partial lnN_P$ was equal to FIE_N

[b]R^2 represented correlation coefficient

Comment D:

Accounting for the role of topography on cloud droplet formation (Romakkaniemi et al., 2017).

Response: Winds along the slope of the hill would cause upward motion (v_{up}) and further affect the microphysical properties of clouds (Romakkaniemi et al., 2017). We calculated the updraft velocity as shown in the response of Comment B and estimate the sensitivity of drop number concentration (N_C) to v_{up} ($S(v_{up})=\partial ln\ N_c/\partial lnv_{up}$) as shown in Table S2. Compared with CP-1 which was formed under relatively clean conditions, CP-2 was more sensitive to the change of v_{up}. We added the corresponding discussion in Page 10 Line 28 to Page 11 Line 6:

"In addition, the meteorological conditions and the topography during the monitoring period would also affect the microphysical properties of clouds. The sensitivity analysis of N_C to CBH and v_{up} was estimated by applying the equation as $S(X_i)=\partial lnN_C/\partial lnX_i$, where X_i represented CBH and v_{up}. As shown in Talbe S2, CP-2 was more sensitive to the variation of meteorological parameters if compared with CP-1. It was consistent with the study of McFiggans et al. (2006). They found that the sensitivity of N_C to v_{up} increased while the sensitivity of N_C to N_P decreased when N_P > 1000 # cm^{-3}. In the present study, the higher values of FIE_r and FIE_N of CP-1 indicated that if the same amount of aerosol particles entered the cloud, the size of cloud droplets in CP-1 would decrease more than that in CP-2. The albedo during CP-1 would be more susceptible to the change of aerosol particles. While the higher values of S(CBH) and S(v_{up}) of CP-2 indicated that CP-2 was more sensitive to the change of CBH and v_{up}. It might cause the periodical variations of cloud microphysical properties during CP-2."

Table S2. Estimated updraft velocity (V_{up}) (means ± S.D.), estimated cloud base height (CBH) (means ± S.D.) and the sensitivities analysis of N_C to N_P, CBH and v_{up} during CP-1 and CP-2.

	V_{up} m s^{-1}	CBH m	$^{a,b}\partial lnN_C/\partial lnN_P(R^2)$	$^{b}\partial lnN_C/\partial lnCBH(R^2)$	$^{b}\partial lnN_C/\partial lnv_{up}(R^2)$
CP-1	0.82 ± 0.29	1017.9 ± 301.5	0.544(0.2820)	-0.118(0.0018)	0.275(0.0599)
CP-2	0.92 ± 0.36	1040.4 ± 260.2	0.144(0.0500)	0.216(0.1279)	0.868(0.1167)

[a]The value of $\partial lnN_C/\partial lnN_P$ was equal to FIE_N

[b]R^2 represented correlation coefficient

Comment E:

A more robust isolation of anthropogenic pollution using either air-mass back trajectory based approaches such as Tunved et al., 2013, or chemical composition analysis if available.

Response: Thank you for your comment. We added the information of inorganic compositions of cloud samples in the revised manuscript (Fig. S4). During each of CP-1 and CP-2, 12 cloud samples were collected. As shown in Fig. S4, the ion compositions of cloud samples during CP-1 and CP-2 were similar. Secondary inorganic species (sulfate, nitrate and ammonia) were dominant ions in cloud. The sum of these three ions accounted for 93.39% and 90.37% of the total measured ions for cloud samples collected during CP-1 and CP-2. It represented that CP-1 and CP-2 were influenced by anthropogenic pollutions from same sources. (Page 8 Line 17-20)We added this information in Page 8 Line 17 - 20. What's more, the chemical compositions of cloud samples will be focused in our next paper.

"For cloud water samples collected during CP-1 and CP-2, the percentage of chemical compositions did not change a lot (Fig. S4). Three dominant main anions (sulfate, nitrate and ammonia) accounted for 93.39% in CP-1 and 90.37% in CP-2 of the total measured ions. The high concentration of secondary ions in the cloud water samples indicated that clouds at Mt. Tai were dramatically influenced by anthropogenic emissions."

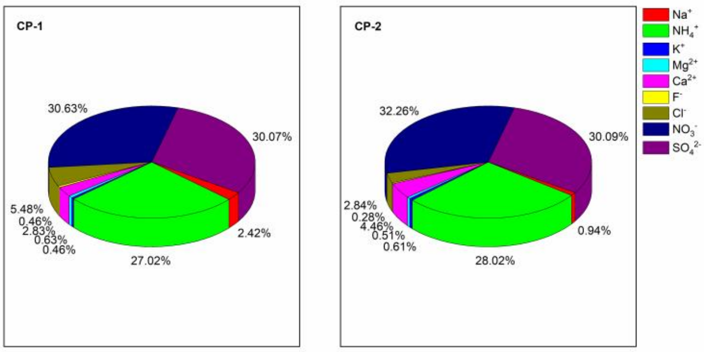

Figure S4. The averaged inorganic chemical compositions of cloud samples collected during CP-1 and CP-2. Each cloud process contained 12 cloud samples.

Furthermore, PM2.5 is not the appropriate measurement to separate aerosol conditions to investigate ACI. Please use an appropriate measure of the aerosol physical properties.

Response: In Figure 3, we had already put the information of N_P. It represented that CE-19 and cloud events in CP-2 (CE-20 to CE-26) started with different N_P. In the revised manuscript as shown in section 3.2, we combined $PM_{2.5}$ and N_P together to identify aerosol conditions of CP-1 and CP-2 (Page 8 Line 8 - 17).

"Two typical cloud processes were selected and analysed with their special characteristics. In cloud process-1 (CP-1, including one cloud event – CE-19), cloud droplets formed under a relatively stable (wind speed < 4 m s^{-1}) and clean ($PM_{2.5} \approx 10.9$ μg m^{-3}, $N_P \approx 1425$ # cm^{-3}) conditions accompanied by a slow increase of T_a (Fig. 2, Fig. 3). During daytime, especially in the afternoon, the $PM_{2.5}$ mass concentration dramatically increased with little change in wind speed and wind direction and N_P could reach to about 5000 # cm^{-3} (Fig. 3). However, the perturbation of particles did not break off the cloud, which made CP-1 be the longest cloud process and persist 74 hours in the present study. Quite different from CP-1, cloud process-2 (CP-2) contained eight cloud events (CE-20 to CE-26, Fig. 3) and occurred periodically under high $PM_{2.5}$ (Fig. 2, 50.7 μg m^{-3} in average) as well as high N_P (Fig. 3, 1694 # cm^{-3} in average) conditions. Cloud events in CP-2 formed after sunset with sharp decreasing of $PM_{2.5}$ and N_P, and transitorily dissipated at noon accompanied with the increase of $PM_{2.5}$, N_P, T_a and cloud base height (CBH)."

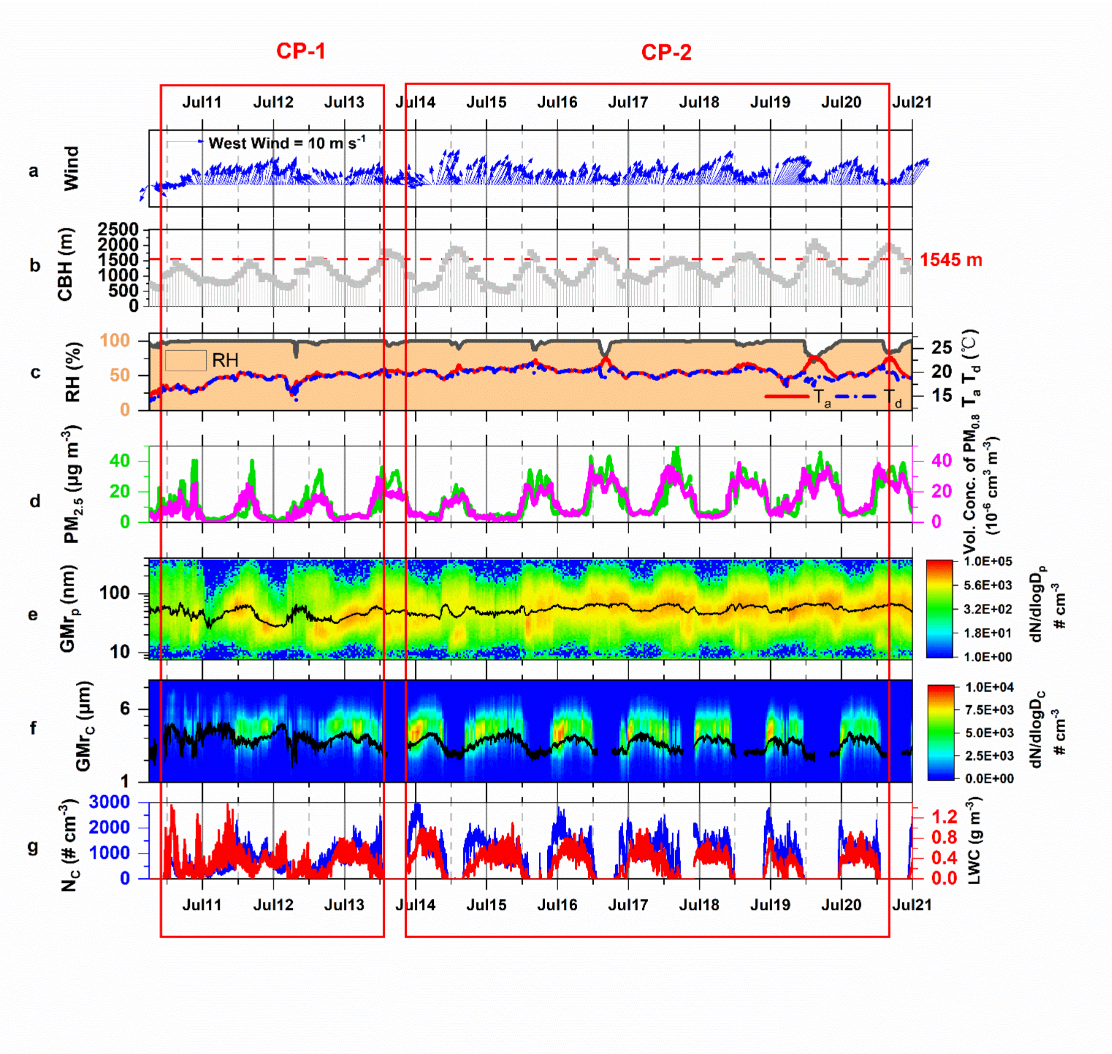

Figure 2: The monitoring information of CP-1 and CP-2. Including (a) Wind speed (WS, m s^{-1}) and wind direction (WD), (b) cloud based height (CBH, m) (c)relative humidity (RH, %), ambient temperature (T_a, ℃) and dew point temperature (T_d, ℃) (d) $PM_{2.5}$ mass concentrations (μg m^{-3}) and volumn concentration of $PM_{0.8}$ (10^{-6} cm^3 cm^{-3}) (e) size distribution of particles (13.6-763.5 nm) and corresponding geometric mean radius (GMr_P) (f) size distribution of cloud droplets (2-50 µm) and corresponding geometric mean radius (GMr_C) (g) N_C and LWC of cloud droplets.

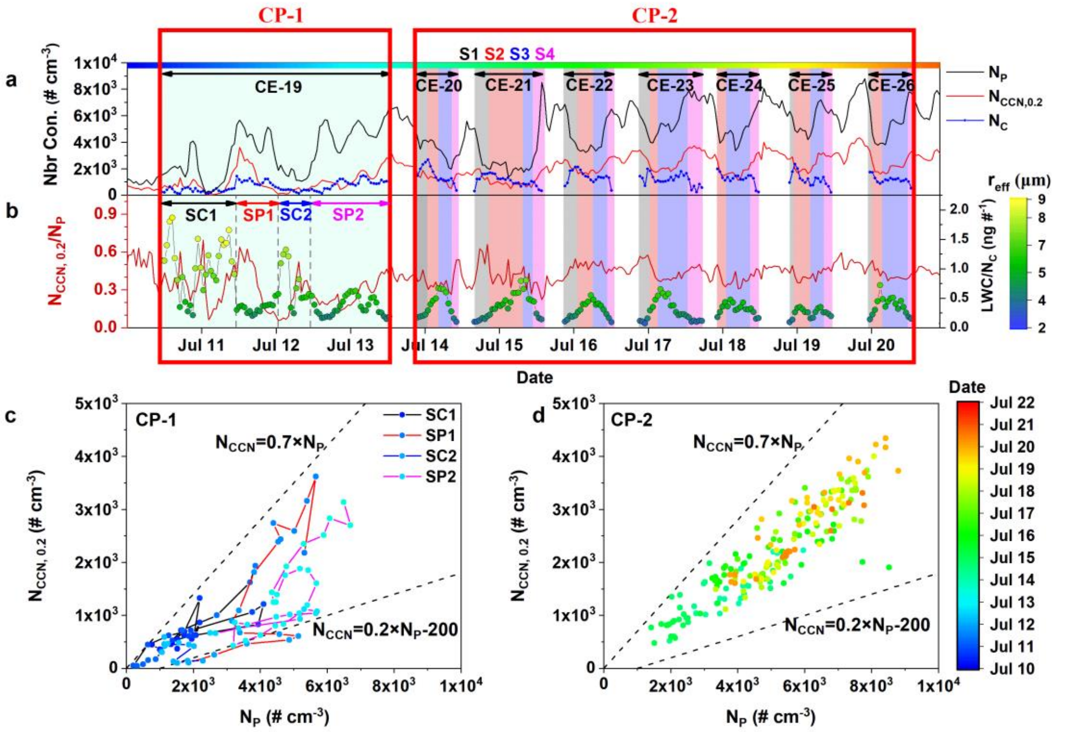

Figure 3: Variation of (a) N_C, N_P and $N_{CCN,0.2}$ (b) $N_{CCN,0.2}/N_P$ and LWC/N_C during CP-1 and CP-2. The plot of $N_{CCN,0.2}$ versus N_P (c) in CP-1 (d) in CP-2. The two dashed lines are the visually defined boundaries from the study of Asmi et al. (2012).

Comment F:

A discussion of the role of wind direction on the reliability of measurements of cloud properties from the Fog monitor, see discussion on cloud droplet measurements in Leskinen et al., 2009 as well as a detailed description of any corrections performed to the measured parameters and uncertainties associated with sampling methods.

Response: Even though the Fog Monitor was installed in a fixed position during our monitoring program, it faced the prevailing wind direction. The ambient wind direction would affect the sampling angle and further influence the sampling efficiency of Fog Monitor. The influence of wind direction on Fog Monitor during CP-1 and CP-2 was evaluated based on the studies of Hammer et al. (2014) and Spiegel et al. (2012). Please check the detailed calculation process in the response of Comment B. Through estimating the sampling angle and the R_V during CP-1 and CP-2, the sampling efficiency was almost equal to 1. Thus, we assumed that the influence of wind direction on Fog Monitor during CP-1 and CP-2 was small and could be ignored in the present study.

Comment G:

Justification of choice of metrics, e.g. CCN at 0,2% supersaturation and others not commonly employed in ACI process studies, e.g.: Nccn(0.2)/Np. Why did you not focus on the droplet activated fraction (Nc/Np)?

Response: In many previous studies, CCN at 0,2% supersaturation has been selected to discuss aerosol-cloud interactions (such as the studies of Jia et al. (2019) and Zheng et al. (2011)). In the atmosphere, not all particles can be act as cloud condensation nuclei and form cloud droplets. In the present study, we used N_{CCN}/N_P instead of N_C/N_P to represent the activation properties of particles. It is applied to characterize the activation ability of particles before CP-1 and CP-2. In addition, we discussed about the relationship between N_C and N_P as shown in Page 9 Line 17 - 28. Both positive and negative relations between N_P and N_C have been observed and they appeared at different cloud processes and at different stages of cloud events.

"Within the present study, both positive and negative relations between N_P and N_C have been observed. But they appeared at different cloud processes (e.g., N_P and N_C showed consistent variation in CP-1) and at different stages of cloud events (e.g., an obviously inverse relation between N_P and N_C existed in S1 and S4 while N_P and N_C simultaneously decreased in S2) (Fig. 3a). High LWC/N_C value indicating water was sufficient for new cloud droplet formation. Once N_P increased, part of the cloud water was taken away by the CCN in the particles to form new droplets, and the remaining amount of water was still sufficient to maintain the previous droplets in liquid state. Positive relationship was existed between N_P and N_C. However, lower LWC/N_C values, to some extent, limited the formation of new cloud droplets. The activated particles grew at the beginning of the cloud cycle would lower the surrounding supersaturation and to some extent limit further aerosol activation (Ekman et al., 2011). The part of water taken by the CCN in the particles was not enough to active all of them to be new droplets and the remaining amount of water was also insufficient to maintain all the previous droplets in liquid state. Then the N_C would decrease and the more the Np, the sharper decrease the N_C. Thus, the inverse relationship would be observed."

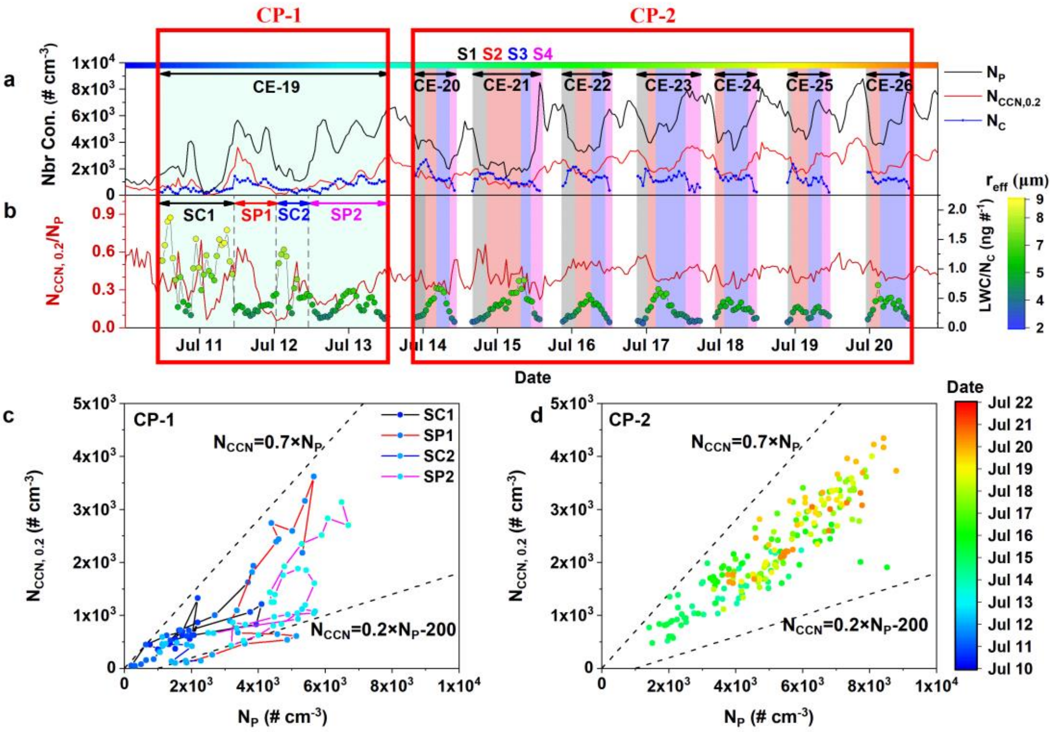

Figure 3: Variation of (a) N_C, N_p and $N_{CCN,0.2}$ (b) $N_{CCN,0.2}/N_P$ and LWC/N_C during CP-1 and CP-2. The plot of $N_{CCN,0.2}$ versus N_P (c) in CP-1 (d) in CP-2. The two dashed lines are the visually defined boundaries from the study of Asmi et al. (2012).

Comment H:

In light of the new analysis associated with (A-G) a newly revised, clear explanation of cloud processes using the observations. Conclusions should not be presented as fact unless they are fully supported by the observations in the manuscript.

Response: The cloud processes were clearly explained based on the comments from two reviewers (Page 8 Line 21 to Page 9 Line 8). Our conclusions were presented based on the observation program at Mt. Tai. We carefully checked them and presented them in the revised manuscript.

"CP-1 was separated into four stages, including SC1 (stage-clean 1), SP1 (stage-perturbation 1), SC2 (stage-clean 2), and SP2 (stage-perturbation 2) based on whether the perturbation of particles occurred (Fig. 3b). The characteristics of SC1 and SC2 were low N_C (383 # cm^{-3} and 347 # cm^{-3}, respectively), large r_{eff} (7.26 μm and 6.36 μm, respectively) and high LWC/N_C (1.01 ng $\#^{-1}$ and 0.75 ng $\#^{-1}$, respectively, which represents averaged water each cloud droplet contained) (Fig. 3b). During SP1 and SP2, the perturbation through particles occurred. Dramatic increase of N_C (949 # cm^{-3} and 847 # cm^{-3}, respectively) and decrease of r_{eff} (4.90 μm and 4.88 μm, respectively) and LWC/N_C (0.35 ng $\#^{-1}$ and 0.36 ng $\#^{-1}$, respectively) was caused.

Each cloud event of CP-2 was separated into activation stage (S1), collision-coalescence stage (S2), stable stage (S3), and dissipation stage (S4) according to the regular changes of N_C and LWC/N_C (Fig. 3a). In S1, N_C dramatically increased to its maximum value among the cloud events. In S2, N_C declined sharply to a stable value, meanwhile LWC/N_C reached the maximum value. In S3, N_C was stable or slightly varied and LWC/N_C started to decrease. In S4, both N_C and LWC/ N_C decreased sharply again and finally arrived zero. Even though the two stages (S2 and S3) in CE-25 were not totally follow the division rules, the other six cloud events followed well. It indicated that the division was helpful to study the variations of cloud microphysical properties during CP-2. The newly formed cloud droplets during S1 were characterized by small size, high N_C and low LWC/N_C values (Fig. 2f and 3b). For example, about 2310 # cm^{-3} of cloud droplets can quickly form in the first 2 hours of CE-20. The r_{eff} of these droplets was smaller than 4.1 μm and LWC/N_C was about 0.2 ng $\#^{-1}$. In going from S2 to S3, the strong collision-coalescence between cloud droplets caused the increase of both r_{eff} and LWC/N_C. In S4, the increase of $PM_{2.5}$, N_P and T_a (Fig. 2b and Fig. 2c) decreased cloud droplet sizes (Rosenfeld et al., 2014a), decreased the ambient supersaturation, enhanced the evaporation of small droplets (Ackerman et al., 2004), and finally caused the vanishment of cloud events (Mazoyer et al., 2019)."

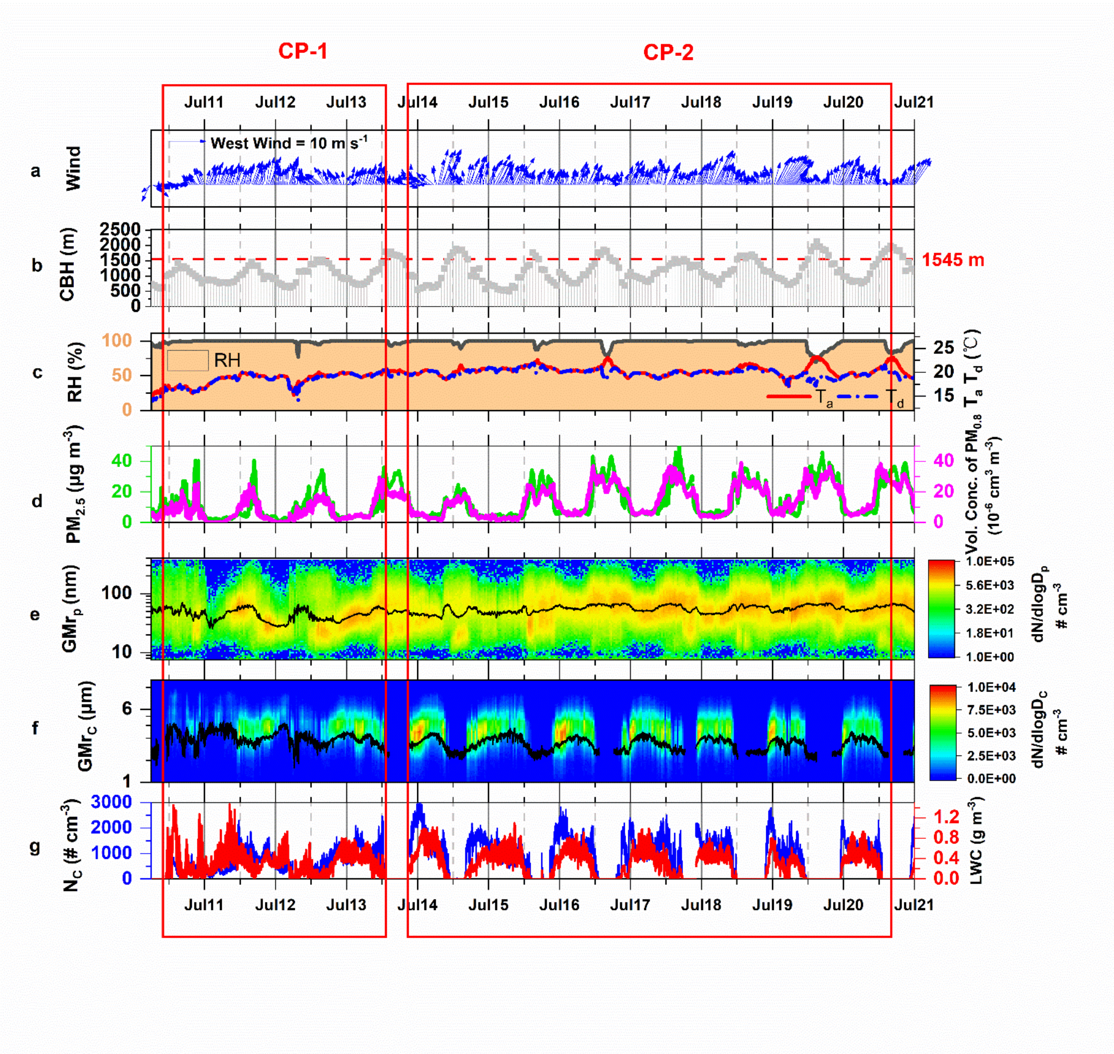

Figure 2: The monitoring information of CP-1 and CP-2. Including (a) Wind speed (WS, m s^{-1}) and wind direction (WD), (b) cloud based height (CBH, m) (c)relative humidity (RH, %), ambient temperature (T_a, ℃) and dew point temperature (T_d, ℃) (d) $PM_{2.5}$ mass concentrations (μg m^{-3}) and volumn concentration of $PM_{0.8}$ (10^{-6} cm^3 cm^{-3}) (e) size distribution of particles (13.6-763.5 nm) and corresponding geometric mean radius (GMr_P) (f) size distribution of cloud droplets (2-50 μm) and corresponding geometric mean radius (GMr_C) (g) N_C and LWC of cloud droplets.

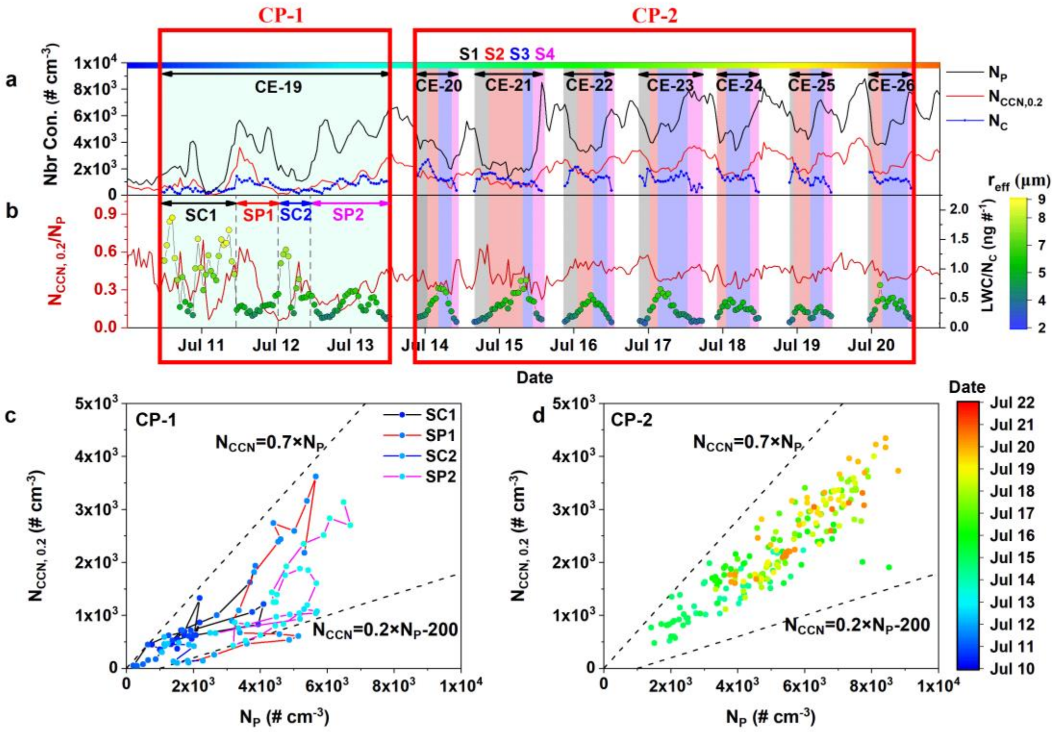

Figure 3: Variation of (a) N_C, N_P and $N_{CCN,0.2}$ (b) $N_{CCN,0.2}/N_P$ and LWC/N_C during CP-1 and CP-2. The plot of $N_{CCN,0.2}$ versus N_P (c) in CP-1 (d) in CP-2. The two dashed lines are the visually defined boundaries from the study of Asmi et al. (2012).

Comment I:

A detailed explanation of how cloud top albedo was calculated including any assumptions made and a discussion as to their validity. An assumption is made related to the calculation of cloud liquid water path, e.g. Stephens, 1978 that is not discussed.

Response: Thank you for your comment. In the study of Stephen et al. (1978), the assumption related to the calculation of cloud liquid water path is that the cloud is vertically uniform with respect to droplet size distribution. We added the description of this assumption in Section 2.8 in the revised manuscript (Page 7 Line 4 - 8):

"Cloud albedos can be calculated using the equations shown below (Seinfeld and Pandis, 2006). Assuming the cloud droplet size distribution can be approximated as monodisperse and the cloud is vertically uniform with respect to droplet size distribution (Stephens, 1978), the cloud optical thickness (τ_c) could be obtained by

$$\tau_c = h\left(\frac{9\pi LWC^2 N_c}{2\rho_w^2}\right)^{\frac{1}{3}}$$

Where h is the thickness of the cloud and ρ_w is the density of cloud water."

Is the assumption of 100m cloud depth valid? Furthermore, it appears that this calculation might be inconsistent as cloud top measurements of cloud microphysical properties are not provided.

Response: Based on the equations in Section 2.8, albedo depends on the values of LWC, N_C and cloud thickness. Here, we set the same cloud thickness for CP-1 and CP-2, and discuss the change of the albedo due to the variations of LWC and N_C. Unfortunately, we don't have the corresponding data of cloud thickness during our monitoring program. In the revised manuscript, we applied the averaged values of LWC and N_C of CP-1 and CP-2 to calculate the corresponding albedo during CP-1 and CP-2 with the change of cloud thickness (Fig. 6d). For a given cloud thickness, albedo during CP-2 was always higher than that during CP-1 if the cloud thickness is lower than about 2500 m (Fig. 6d). We revised this part in Page 13 Line 19 - 24.

"The thickness of orographic cloud was usually very thin (Welch et al., 2008). If assuming the cloud thickness during CP-1 and CP-2 were equal, albedo would depend on the values of LWC and N_C as described in Section 2.8. Cloud albedo during CP-2 was always higher than that during CP-1, especially when the cloud thickness was lower than about 2500 m (Fig. 6d). Through studying marine stratocumulus clouds in the north-eastern Pacific Ocean, Twohy et al. (2005) also found that the increase of N_C by a factor of 2.8 would lead to 40% increase of albedo going from 0.325 to 0.458. It indicated that the higher N_C would increase the cloud albedo if assuming no change of cloud thickness."

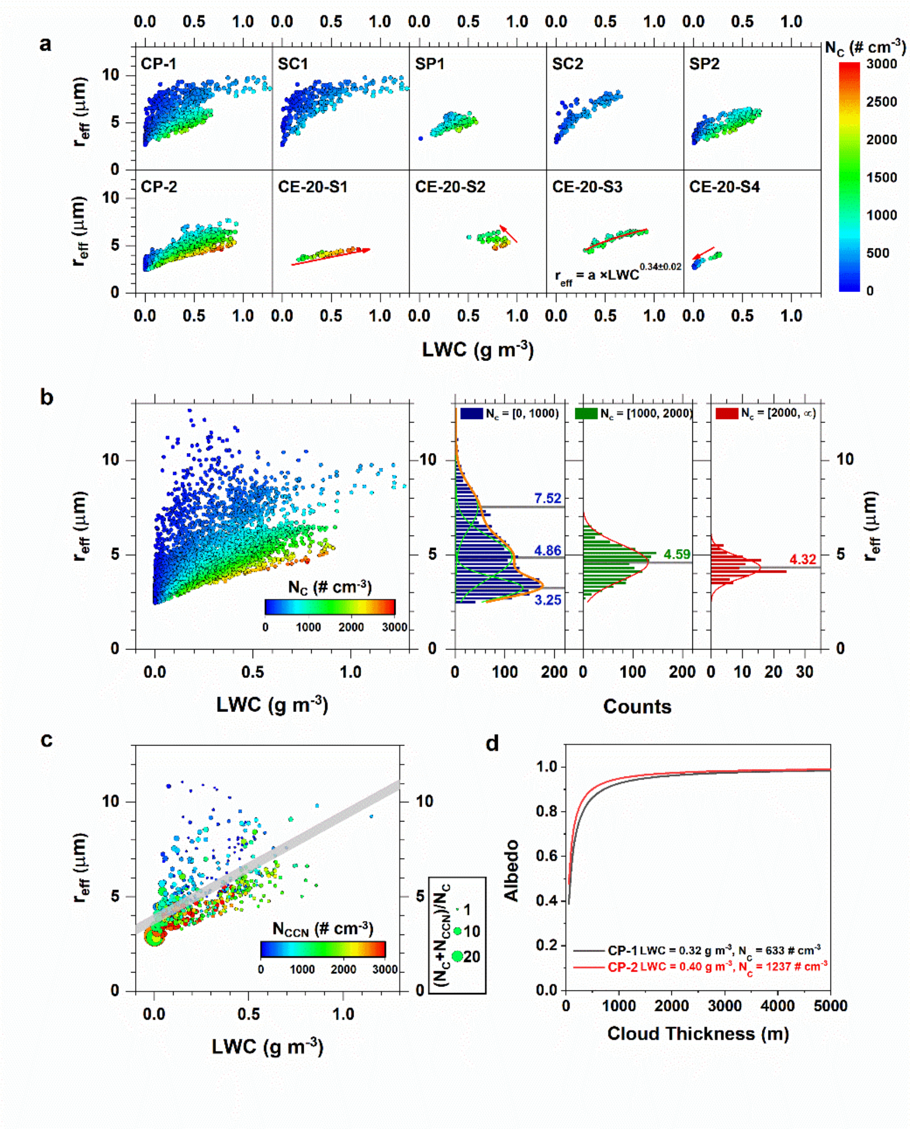

Figure 6: The plot of LWC versus r_{eff} (a) in different cloud stages of CP-1 and CP-2 (b) under different N_C ranges (c) under different N_{CCN}. The time resolution of the corresponding data was 5 min in (a), (b) and 50 min in (c). (d) The plot of albedo versus the variation of cloud thickness during CP-1 and CP-2. The averaged values of LWC and N_C of CP-1 and CP-2 were applied to calculate albedo according to the equations in Section 2.8.

Reference

Ackerman, A. S., Kirkpatrick, M. P., Stevens, D. E., and Toon, O. B.: The impact of humidity above stratiform clouds on indirect aerosol climate forcing, Nature, 432, 1014-1017, 10.1038/nature03174, 2004.

Asmi, E., Freney, E., Hervo, M., Picard, D., Rose, C., Colomb, A., and Sellegri, K.: Aerosol cloud activation in summer and winter at puy-de-Dome high altitude site in France, Atmos. Chem. Phys., 12, 11589-11607, 10.5194/acp-12-11589-2012, 2012.

Ekman, A. M. L., Engstrom, A., and Soderberg, A.: Impact of Two-Way Aerosol-Cloud Interaction and Changes in Aerosol Size Distribution on Simulated Aerosol-Induced Deep Convective Cloud Sensitivity, J. Atmos. Sci., 68, 685-698, 10.1175/2010jas3651.1, 2011.

Georgakakos, K. P., and Bras, R. L.: A hydrologically useful station precipitation model. I. Formulation, Water Resources Research, 20, 1585-1596, 10.1029/WR020i011p01585, 1984.

Hammer, E., Bukowiecki, N., Gysel, M., Juranyi, Z., Hoyle, C. R., Vogt, R., Baltensperger, U., and Weingartner, E.: Investigation of the effective peak supersaturation for liquid-phase clouds at the high-alpine site Jungfraujoch, Switzerland (3580 m a.s.l.), Atmospheric Chemistry and Physics, 14, 1123-1139, 10.5194/acp-14-1123-2014, 2014.

Hudson, J. G.: Variability of the relationship between particle size and cloud-nucleating ability, Geophys. Res. Lett., 34, 10.1029/2006gl028850, 2007.

Jia, H. L., Ma, X. Y., and Liu, Y. G.: Exploring aerosol-cloud interaction using VOCALS-REx aircraft measurements, Atmospheric Chemistry and Physics, 19, 7955-7971, 10.5194/acp-19-7955-2019, 2019.

Mazoyer, M., Burnet, F., Denjean, C., Roberts, G. C., Haeffelin, M., Dupont, J. C., and Elias, T.: Experimental study of the aerosol impact on fog microphysics, Atmos. Chem. Phys., 19, 4323-4344, 10.5194/acp-19-4323-2019, 2019.

Romakkaniemi, S., Maalick, Z., Hellsten, A., Ruuskanen, A., Vaisanen, O., Ahmad, I., Tonttila, J., Mikkonen, S., Komppula, M., and Kuhn, T.: Aerosol-landscape-cloud interaction: signatures of topography effect on cloud droplet formation, Atmospheric Chemistry and Physics, 17, 7955-7964, 10.5194/acp-17-7955-2017, 2017.

Rosenfeld, D., Andreae, M. O., Asmi, A., Chin, M., de Leeuw, G., Donovan, D. P., Kahn, R., Kinne, S., Kivekas, N., Kulmala, M., Lau, W., Schmidt, K. S., Suni, T., Wagner, T., Wild, M., and Quaas, J.: Global observations of aerosol-cloud-precipitation-climate interactions, Rev. Geophys., 52, 750-808, 10.1002/2013rg000441, 2014a.

Seinfeld, J. H., and Pandis, S. N.: Atmospheric Chemistry and Physics: From Air Pollution to Climate Change, John Wiley & Sons, Inc., Hoboken, New Jersey, 2006.

Shen, L., Wang, H., Yin, Y., Chen, J., and Chen, K.: Observation of atmospheric new particle growth events at the summit of mountain Tai (1534 m) in Central East China, Atmos. Environ., 201, 148-157, 10.1016/j.atmosenv.2018.12.051, 2019.

Spiegel, J. K., Zieger, P., Bukowiecki, N., Hammer, E., Weingartner, E., and Eugster, W.: Evaluating the capabilities and uncertainties of droplet measurements for the fog droplet spectrometer (FM-100), Atmospheric Measurement Techniques, 5, 2237-2260, 10.5194/amt-5-2237-2012, 2012.

Stephens, G. L.: Radiation profiles in extended water clouds. II. Parameterization schemes, Journal of the Atmospheric Sciences, 35, 2123-2132, 10.1175/1520-0469(1978)035<2123:Rpiewc>2.0.Co;2, 1978.

Twohy, C. H., Petters, M. D., Snider, J. R., Stevens, B., Tahnk, W., Wetzel, M., Russell, L., and Burnet, F.: Evaluation of the aerosol indirect effect in marine stratocumulus clouds: Droplet number, size, liquid water path, and radiative impact, J. Geophys. Res.: Atmos., 110, -, 2005.

Verheggen, B., Cozic, J., Weingartner, E., Bower, K., Mertes, S., Connolly, P., Gallagher, M., Flynn, M., Choularton, T., and Baltensperger, U.: Aerosol partitioning between the interstitial and the condensed phase in mixed-phase clouds, Journal of Geophysical Research-Atmospheres, 112, 13, 10.1029/2007jd008714, 2007.

Welch, R. M., Asefi, S., Zeng, J., Nair, U. S., Han, Q., Lawton, R. O., Ray, D. K., and Manoharan, V. S.: Biogeography of tropical montane cloud forests. Part I: Remote sensing of cloud-base heights, Journal of Applied Meteorology and Climatology, 47, 960-975, 10.1175/2007jamc1668.1, 2008.

Zheng, X., Albrecht, B., Jonsson, H. H., Khelif, D., Feingold, G., Minnis, P., Ayers, K., Chuang, P., Donaher, S., Rossiter, D., Ghate, V., Ruiz-Plancarte, J., and Sun-Mack, S.: Observations of the boundary layer, cloud, and aerosol variability in the southeast Pacific near-coastal marine stratocumulus during VOCALS-REx, Atmos. Chem. Phys., 11, 9943–9959, https://doi.org/10.5194/acp-11-9943-2011, 2011.